

# First Supernovae and Heavy Elements

Robert Canevy

February 2023

## Abstract

In this project, the metallicity profiles and mixing of metals in the IGM surrounding and within a target halo are investigated. Using a magnetohydrodynamical based model solved by Enzo, an analysis pipeline was constructed, aided by the libraries of yt and ytree, to determine 50 profiles of mass weighted fields. Four of which; metallicity, vortical time, dynamical time and cooling time were developed as a function of radius to explore the enrichment mechanism occurring, at a given distance from the centre of the halo, and the efficiency of mixing for each mechanism. The profiles agree and conclude that as redshift decreases, from the perspective of the target halo, external enrichment (EE) [1] is indeed the dominant mechanism with very efficient turbulent-driven mixing taking place.

# Contents

<b>1</b>	<b>Introduction</b>	<b>3</b>
<b>2</b>	<b>Chemical Enrichment</b>	<b>5</b>
2.1	Metallicity from External Enrichment . . . . .	5
2.2	PISNe . . . . .	5
2.3	Timescale Collapse and Mixing . . . . .	6
2.4	Diffusion Process . . . . .	6
2.5	Shock Waves . . . . .	7
2.6	Pre Enrichment . . . . .	7
2.7	Distinguishing POP II from POP II formation . . . . .	8
2.8	The Dominant path . . . . .	8
<b>3</b>	<b>Working with Enzo</b>	<b>8</b>
3.1	Eulerian Equations . . . . .	8
3.2	Radiative Transfer . . . . .	9
<b>4</b>	<b>Python Models</b>	<b>9</b>
4.1	Basic Slice without sphere . . . . .	9
4.2	Multiple slices and radial profiles using pythons 'glob' . . . . .	10
<b>5</b>	<b>Ytree</b>	<b>13</b>
5.1	Analysis Pipeline . . . . .	13
<b>6</b>	<b>Analysis Pipeline Results</b>	<b>18</b>
6.1	Metallicity Profiles . . . . .	18
6.2	Vortical Time . . . . .	19
<b>7</b>	<b>Discussion</b>	<b>19</b>
<b>8</b>	<b>Conclusion</b>	<b>20</b>

# 1 Introduction

Around 50 - 1000 Myrs post Big Bang, the very first stars, population three (POP III) stars had formed within density perturbations in the early Universe [2]. Surrounded by dark matter minihalos (MH), the POP III is theorized to end its life in a Supernova (SN) explosion ejecting gas with the first metals in to the Intergalactic Medium (IGM) as a shock wave enriching neighbouring halos with metals (external enrichment or EE). In other circumstances the gas can also fall back into the MH through a process known as internal enrichment (IE) of metals in the MH. Within the centre of this collapsed region, the cloud cools from its molecules through the formation of hydrogen. The dust grains of the gas induce radiative cooling as they act as black-body emitters colliding with the existing hydrogen molecules at a rate sufficient for thermal coupling to occur. Aided by turbulence caused by the virialization of the halo and collision with the blast-wave, this allows metals to reach the interior of the halo [3]. Knots originating from the dust thermal emission cooling form in the centre of the MH, which further develops and leads to the formation of Extremely Metal Poor (EMP) Stars of metallicity  $[\text{Fe}/\text{H}]$  less than 3 [4] that are observed today in our Galactic Halo [5].

The SNe explosions that ended the lives of the first stars were responsible for the initial enrichment of the IGM with heavy elements. The initial conditions for POP III star formation, as given by variants of the cold dark matter cosmology [6], the number of atomic and molecular transitions increases raising its ability to cool. They are initially massive metal-free gas clouds that cool, fragment and collapse above a given redshift ( $Z$ ) [2]. Descending from these, POP II stars, transition from POP III from certain scenarios, one such way is via chemical enrichment (IE EE) [2]. POP II stars with lower characteristic masses form when the star-forming gas reaches a range in critical metallicity  $Z_{\text{crit}}$  of  $10^{-6}$  -  $10^{-3.5} Z_{\odot}$ . SNe from Pop III stars provide the necessary heavy elements for the transition to a Pop II stellar population. It only takes one, at most two, SNe from Pop III stars in the halo progenitors to complete the transition to Pop II [7]. EE occurring when the halo binding energy is sufficiently below the SN explosion energy [4].

*Smith et al* predicted that over half of the observed metal enriched halos originate from POP III SNe outside of their virial radii. Leading to an important result that occurrence of POP II stars form from the EE mechanism. EE depends on the average separation of the mini halos, and the POP III star formation [3]. This can be explored, for example *Smith et al*, the distance between the Pop III halo and an observed larger halo was found to be around 500pc between, was marginally more than 1 standard deviation lower than the average pair separation within the volume of the simulation. This indicates that the EE mechanism is an important component of how low-metallicity stars develop formation [3].

The primordial Initial Mass Function (IMF) is the distribution of stars as a function of mass in star forming regions stars formed from metal-free gas. The IMF is the most important factor for modelling early enrichment as it can control the mass budget of metals released between stars and the mass distribution of lower mass stars existing at  $Z = 0$ . However nucleosynthetic features uniquely associated with a particular mass range can powerfully constrain the first-stars IMF. The IMF of the first stars was peaked in the range of massive stars that experience core-collapse supernovae [8]. The metallicity of a star is defined as the proportion of chemical elements heavier than helium. Metallicity is often denoted by “ $[\text{Fe}/\text{H}]$ ” here we denote it as “ $Z$ ”, the logarithm of the ratio of iron abundance compared to the iron abundance in the Sun. Iron is used as a reference because it is easy to identify with spectral data in the visible spectrum [9]. To gain further access into the role of the IMF, *Smith et al* [3] found halos surrounding a POP III star had metallicities with corresponding mass  $10 - 2M_{\odot}$  which indicates stars exist with only moderately metal poor yet still pose a single progenitor. With this, the POP III IMF can be further observed further developing knowledge of their distribution.

At the end of the POP IIIs life the shock wave produced can be analysed. Such analysis by Planelles et al [10] performed an analysis of the propagation speed and size of the shock waves developing around MHs further discovering information regarding the formation time and many other main features regarding MHs.

[10]. They had found and proved a correlation between the external shocks surrounding clusters and galaxies and the MHs where such shock waves originate. They collected slices, see section 4.1 for a basic slice, for shock waves between  $z = 1.4 - 0$  distributed around a dominant halo, following the shock wave pattern, dark matter halo position and size. When the  $z$  was 0 they identify the shock wave, then by assuming that the formation of the accretion shock is the formation time of the halo, the formation time of the galaxy cluster can be traced.

But how do these shock waves spread metals into the IGM? The shock waves have been found to have a density of just under  $1\text{cm}^3$  and catches up with the expanding shell of the hydrogen region within a few million years of the explosion. This collision enhances the density by a factor of roughly 10 to 30, after which the shell proceeds to break up into small knots. These knots eventually dissolve carrying metals out into the intergalactic medium [3].

The direction of this project is to investigate the mechanisms (IE, PE or EE) that populate the IGM with metals, and to which extent does the mixing of such metals display efficiency. To further construct dark matter merger trees via Enzo simulations of selected dominant-in-mass halos, analyse correlations between these halos by constructing metallicity profiles.

## 2 Chemical Enrichment

### 2.1 Metallicity from External Enrichment

In this chapter, the investigations into different enrichment mechanisms used in the past are explored.

*How rare is it for a star to form from External Enrichment?* The number of halos externally enriched by POP III SNe varies greatly but if the conditions are right for the EE mechanism to occur, it should typically produce metal-enriched stars before they can form from fallback of metals onto the Pop III halo [3].

The concept of a ‘critical metallicity’ ( $Z_{crit}$ ) has been used to characterize the transition between Population III and Population II formation modes, where  $Z$  denotes the mass fraction contributed by all heavy elements [6]. ( $Z_{crit}$  marks where dust cooling becomes efficient enough to cause fragmentation at high densities. And the regions of high spatial density are where halos are more likely to be enriched externally. The likelihood of the EE mechanism depends on the average separation of Pop III star-forming halos from mini-halos that have yet to undergo star formation [3].

From *Hicks et al* [1] using a simulation to uniquely track metals ejected from POP III stars, the origin of the metals within the metal-enriched halos can be identified. They found that despite the wide range of metallicities associated, that more than half of the enriched halos source from SNe explosions from POP II stars outside of their virial radii. They found that EE by stars with no metals dominates the enrichment process of halos with virial mass below  $10^6 M_\odot$ . POP II stars forming from external enrichment being a rare occurrence due to the small contribution of low mass halos to the global star formation rate as well as the low metallicities at the centre of the halos, in turn are sourced from metal ejected from outside mixing with the interior. Additional to this, they found that the fraction of EE halos increases over time, that PISNe are the predominant SNe leading to external enrichment of halos.

### 2.2 PISNe

*What is a PISNe?*

A Pair-Instability Supernova (PISNe) is a supernova occurring via pair production; the production of free electrons and positrons colliding between atomic nuclei and gamma rays, reducing the internal radiation pressure of a supermassive star’s core against gravity. This decrease in pressure leads to a partial collapse, which in turn provides a greatly accelerated burning in a runaway thermonuclear explosion, resulting in the star being blown completely apart without leaving a stellar remnant behind [11]. By modelling stellar radiative feedback with adaptive ray tracing, a single PISNe is sufficient to enrich a halo to  $103 Z_\odot$  and to transition to POP II star formation[7].

From *Hicke et al* [1] PISNe contributed the most to the enrichment of the observed IGM of primordial IMF, and were consequently found to be the predominant SN type giving rise to the EE of halos despite being only 8 percent of the Pop III SNe events encountered in the sample [1]. However, a factor to consider, *Wise et al* emphasises that photo-dissociating (a chemical reaction in which molecules of a chemical compound are broken down by photons) exhibit a radiation background that decreases enrichment by PISNe and increases the importance of metal-rich galactic outflows, where only  $10^{4-10^2}$  of PISNe ejecta ends up in (EMP) stars with  $M > 0.9 M_\odot$ .

*Conditions for a Black Hole* *Bromm et al* used an estimator of the protostellar mass  $M_*$  and accretion rate  $M_{acc}$  as  $M_* \sim \int M_{acc} dt$  where  $M_{acc}$  is the ratio of the Jeans mass and the free-fall time, to determine that POP III stars with masses below or above the PISN range  $140 \leq M_* \leq 260 M_\odot$  are predicted to form black holes. However the latter does not contribute a significant quantity of heavy elements into the IGM, since most of the newly synthesized metals will be retained in the black hole. The PISN providing all its heavy element production to the surrounding gas [6]. If the star has a mass in this narrow interval, it will explode as a PISN, leading to the complete disruption of the progenitor. If this enrichment is very uniform,

the transition would occur rather suddenly; if, on the other hand, enrichment would be occurring in random areas, with islands of high-metallicity gas embedded in mostly still pristine material, then the transition would occur in a non-synchronized way, probably occupying a considerable time interval [6].

For the PISN explosion studied by *Bromm et al. (2003)*, the extent of the metal enriched region, with a physical size of  $\sim 1\text{kpc}$ , is comparable to the radius of the relic hydrogen region around a MH. In a related paper by *Yoshida et al. 2004*, it is argued that if POP III stars led to an early partial reionization of the universe, as may be required by the recent WMAP results, this will have resulted in a nearly uniform enrichment of the universe to a level  $Z_{min} \geq 10^{-4}Z_{\odot}$  [6].

Elemental abundances of EMP stars can well be reproduced by the nucleosynthetic models of CCSNe. Interestingly, the stars with elemental abundances consistent with PISN model have not been observed so far. This is considered to be either because the formation rate of extremely massive Pop III stars are intrinsically small, or because the ejecta from PISNe, if exist, can not enrich their host or neighbouring MHs [4].

## 2.3 Timescale Collapse and Mixing

Additional to the distance between halos, two other factors of importance for the occurrence of enrichment are the timescale and mixing. *Smith et al 2015* [3] found that for a POP III SN of  $11.19M_{\odot}$  impacting a halo after a SN explosion that gas exists from zero metallicity up to  $10^{-3}Z_{\odot}$  as spherical shells. Within a few pc of the gas cloud no pristine gas exists with metallicity as high as  $10^{-3}Z_{\odot}$ . Further within the shell at 0.01pc the metallicity is nearly constant. To consider why this occurred, [3] stated the timescale collapse and mixing must be compared. Collapse Timescale:

$$t_{ff} = \sqrt{\frac{3\pi}{32G\rho}} \quad (1)$$

Vortical Time:

$$t_{vort} \approx \frac{2\pi}{|\nabla \times \mathbf{v}|} \quad (2)$$

If the mixing is shorter than the free-fall time within a few pc mixing is found to occur. But within one pc, the free-fall/dynamical time can be shorter than the vortical which causes a collapse at a higher rate than the transport of metals to the interior of the gas, prohibiting enrichment. This rate of collapse can be regulated via the free-fall/dynamical time [3].

## 2.4 Diffusion Process

Metal enrichment takes place efficiently with run-away molecular cooling leading to the first POP III star formation events, and to the following, rapid transition to POP II. Depending on the progression of metal enrichment, the continued suppression of hydrogen cooling by external and internal UV radiation and the ability to trap the entropy produced by the release of gravitational energy, the gas at the centre of the halo forms a supermassive star, a stellar-mass black hole accreting at super-Eddington accretion rates or a compact star-cluster undergoing collisional run-away of massive stars at its centre [12]. As a consequence of the chemical feedback, higher values of  $Z_{crit}$  allow the POP III regime to last a bit longer (at most  $< 810^7\text{yr}$ ) and to pollute more with respect to the lower  $Z_{crit}$ . Metal pollution is a very efficient process and  $Z_{crit}$  is easily reached in less than  $10^8\text{yr}$ . The first sites of metal pollution are clumped and dense star forming regions from which metals are spread away via feedback effects. *Maio et al* predicts that in primordial halos, the enriched gas and pristine gas are similar, that they experience similar star formation feedback effects [13].

Analysis of mixing and radiative feedback via the diffusion process can highlight the potential for a POP II cluster. In 2010, *Greif et al* [14] modelled turbulent mixing as a diffusion process. Diffusion is the movement of particles move from an area of high concentration to an area of low concentration until equilibrium is reached. A distinguishing feature of diffusion is that it results in mixing or mass transport without requiring bulk motion. Also, many functions can be calculated explicitly, in the fields where diffusion has been applied,

it has been used to model phenomena evolving randomly and continuously in time under certain conditions [15]. Analysing this mixing with and without radiative feedback with POP III stars that form from near by MHs, they found that most MHs do not change from interactions with ionizing radiation and SNe remnants, with other MHs enriched to significant levels resulting in the forming POP III stars or POP II stars. At the centre of the recently formed galaxy, uniformly enriched gas is in a state of collapse suggesting the prediction that a POP II cluster will form. First galaxies predicted to be detected this way are expected to contain stellar populations with a low redshift.

The development of radiation hydrodynamical methods that are able to follow gas dynamics and radiative transfer self-consistently is key to the solution of many problems in numerical astrophysics [16]. In regards to the turbulence, the coexistence of cold, pristine-gas inflows and of hot, enriched-gas outflows determines turbulence and hydro instabilities [13]. *Shen et al* found from a study of the IGM using particle hydrodynamic simulations to explore models for metal cooling and turbulent diffusion where galactic winds efficiently enrich the IGM for intermediate halos  $10^{10} - 10^{11} M_{\odot}$ . The metals enhance the cooling allowing warm hot IGM gas to cool in galaxies increasing star formation. The metal diffusion allows wind to mix before escaping, replacing metallicity in the IGM with gas within these halos. Diffusion importantly increases the amount of gas with lower  $Z$  [17] and the cooling rate of the metals depends on their ionization state, which in turn is controlled by ionizing backgrounds [6].

$Z < Z_{crit}$  With  $Z$  below the critical, massive Pop III stars would form again within the halo, however enriching the surrounding IGM with Pop III SNe and ejecting material becomes more difficult [7].

## 2.5 Shock Waves

As mentioned previously, EE consists of shock waves from the SNe enriching neighbouring halos with metals. In distinct cases the ionization front or the SN shock can disrupt the core of the halo, heating and ionizing the gas, leading to metal enrichment. This in turn may trigger the formation less massive Pop III or normal Pop II stars if enough metals are brought to the center of the halo. The amount of fragmentation sensitively depends on the initial conditions of the collapse [14].

## 2.6 Pre Enrichment

Another case of enrichment exists for halos that form within a region of the IGM that has already been enriched. So far, it is assumed that every enriched halo that is not internally enriched is externally enriched by a nearby supernova remnant. However, halos forming in an enriched region of the IGM will accrete gas from the environment during virialization and become enriched that way. This is pre-enrichment. This occurs if their mass-weighted metallicity is  $105.3 Z_{\odot}$ . Only a small percentage of enriched halos form pre-enriched [1]. It is generally believed that MHs can only host Pop III stars, as self-enrichment is unlikely, and transport of metals out of the IGM into pre-condensed halos might be severely limited [14].

*Bromm et al* Explored numerical simulations of the fragmentation process indicating that lower mass stars can only form out of gas that was already pre-enriched to a level in excess of the  $Z_{crit}$ , estimated to be of order  $10^{410^{3Z_{\odot}}}$ . Depending on the nature of the first SNe explosions, and in particular on how efficiently and widespread the mixing of the metal-enriched ejecta proceeds, the cosmic star formation will at some point undergo a fundamental transition from a POP III dominated mode to one dominated by POP II [6].

## 2.7 Distinguishing POP II from POP II formation

It has been suggested that the transition in the star formation mode, from high-mass Pop III to normal-IMF Pop II, occurs once a minimum metal enrichment was in place, the critical metallicity  $Z_{crit} \approx 10^{-4} Z_{\odot}$  [18]. It is therefore significant to identify any high  $Z_{crit}$  regions within a simulation to distinguish between Pop III and Pop II star formation sites.

## 2.8 The Dominant path

EE is conclusively the dominant enrichment pathway that can provide enough metals to push the average metallicity of high redshift MHs above the critical value required for Pop II star formation. Not all halos enriched through this mechanism are massive enough to form stars. When EE does trigger Pop II star formation, the resulting star particles have low metallicity. The fraction of halos that are externally enriched increases over time, and the majority of these halos have virial mass below  $(10^6 M_{\odot})$ . This in contrast to IE being found the dominant pathway for halos forming Pop II stars where most Pop II star formation occurs in the most massive halo.[1].

## 3 Working with Enzo

ENZO is an open-source, adaptive mesh refinement + N-body cosmological simulation code that has been heavily used for simulating cosmological structure formation over a large range of scales. ENZO has been employed by numerous works to study high-redshift structure formation, including Pop III star formation, low metallicity star formation and the first galaxies [3]. It can provide temporal and spatial resolution for models concerning fluidity. In Cartesian coordinates, it runs up to 3 Dimensions supporting a vast library consisting of hydrodynamics, self gravitational fluids, primordial gas chemistry, radiative cooling of primordial and metal enriched plasma, radiation transport, models for star formation and feedback and cosmological expansion. [19].

### 3.1 Eulerian Equations

Enzo utilises Eulers equations of ideal magnetohydrodynamics, a set of equations constructed from the Navier Stokes fluid dynamics and the Maxwellian equations of electromagnetism with gravity in a system comoving with cosmological expansion.

Let  $E, \rho, v, B, I$  denote the comoving total fluid energy density, comoving gas density, peculiar velocity, comoving magnetic field strength, and the Identity matrix respectively and  $a$  as the cosmological expansion. The first three equations are moments of the Boltzmann equation, with the fourth being a magnetic form of the induction equation. The first moment of the Boltzmann is the conservation of mass - the continuity equation [6]:

$$\frac{\partial \rho}{\partial t} + \frac{1}{a} \nabla \cdot (\rho \mathbf{v}) = 0$$

The second defines the conservation of momentum:

$$\frac{\partial \rho v}{\partial t} + \frac{1}{a} \nabla \cdot (\rho \mathbf{v} \mathbf{v} + \mathbf{I} \rho^* - \frac{\mathbf{B} \mathbf{B}}{a}) = -\frac{\dot{a} \rho v}{a} - \frac{\rho \nabla \phi}{a}$$

$\dot{a}$  is how fast the Universe is expanding,  $\nabla \phi$  denotes the gravitational potential that utilises a Fast Fourier Transform to describe how a gas interacts with dark matter particles and the positions of the dark matter particles. With  $\dot{a} = 0, \mathbf{B} = 0, a = 1$  this effectively reduces a box in the simulation to approximately 1, fixed Universe (constant expansion), and can simplify to the conservation of mass [19].

The third being conservation of energy i.e. the kinetic and magnetic fluid energy:



$$\frac{\partial E}{\partial t} + \frac{1}{a} \nabla \cdot [(\mathbf{E} + \mathbf{p}^*)\mathbf{v} - \frac{1}{a} \mathbf{B}(\mathbf{B} \cdot \mathbf{v})] = -\frac{\dot{a}}{a}(2E - \frac{B^2}{2a}) - \frac{\rho}{a} \mathbf{v} \cdot \nabla \phi - \Lambda + \Gamma + \frac{1}{a^2} \nabla \cdot \mathbf{F}_{\text{cond}}$$

And lastly:  $\frac{\partial \mathbf{B}}{\partial t} - \frac{1}{a} \nabla \times (\mathbf{v} \times \mathbf{B}) = 0$  a form of the induction equation [19].

### 3.2 Radiative Transfer

The equation describes how radiation travels, how it absorbs and emits radiation and the energy released via scattering.

In order to describe radiative transfer, Enzo solves an angled averaged radiative transfer equation through flux diffusion with gas energy and chemical number densities. The first to be solved:

$$\frac{\partial E_r}{\partial t} + \frac{1}{a} \nabla \cdot (\mathbf{E}_r \mathbf{v}) = \frac{1}{a^2} \nabla \cdot (\mathbf{D} \nabla \mathbf{E}_r) - \frac{\dot{a}}{a} E_r - ck E_r + \eta$$

with  $E_r$  as the radiation energy density. And the second:

$$\frac{\partial e_c}{\partial t} = -\frac{2\dot{a}}{a} e_c + \Gamma - \Lambda$$

where  $e_c$  denotes the internal energy correction of photo-heating and chemical cooling [19].

## 4 Python Models

### 4.1 Basic Slice without sphere

Before introducing the merger trees analysed using *ytree*, the basics must be explored first. The simulations discussed in the following sections utilizes an open-source python toolkit called 'yt', an analysis tool used with volumetric data [20].

Based on the information from the yt sites: '[yt-project.org/doc/cookbook/](http://yt-project.org/doc/cookbook/)' or simply '*The yt Cookbook*' is the models used in creating the following slices of the clusters in the dataset.

```
import os
import yt
```

```
'''
```

Example of a simple slice of width 80 kpc through the z axis of a gas/density dataset, centered on maximum density.

```
'''
```

```
data_dir = '/disk12/brs/pop2-prime/firstpop2_L2-Seed3-large/pisn_solo/' #location of file
plot_directory = '/home/rcanevy/plots/slices' #location for where slice has to be saved
sample_plot = 'AltSlice_DD0098.png' #name slice in png format
path = os.path.join(data_dir, "DD0098", "DD0098") #path from slice location to saving location
ds = yt.load(path) #loads dataset with path specified
plt = yt.SlicePlot(ds, "z", ("gas", "density"), center=("max", "density"), width=(80.0, "kpc"))
plt.save(os.path.join(plot_directory, sample_plot)) #saves the slice
```

Within a dataset, imagine a three dimensional box of information surrounding the halo, fields (such as gas, temperature) surrounding the point of interest. A slice is essentially cutting through the 3rd axis, the depth of the first two dimensions in question, and provides a section of information at that point within given fields. This cuts through the box of information extended from the two dimensions of gas vs density at a given width.

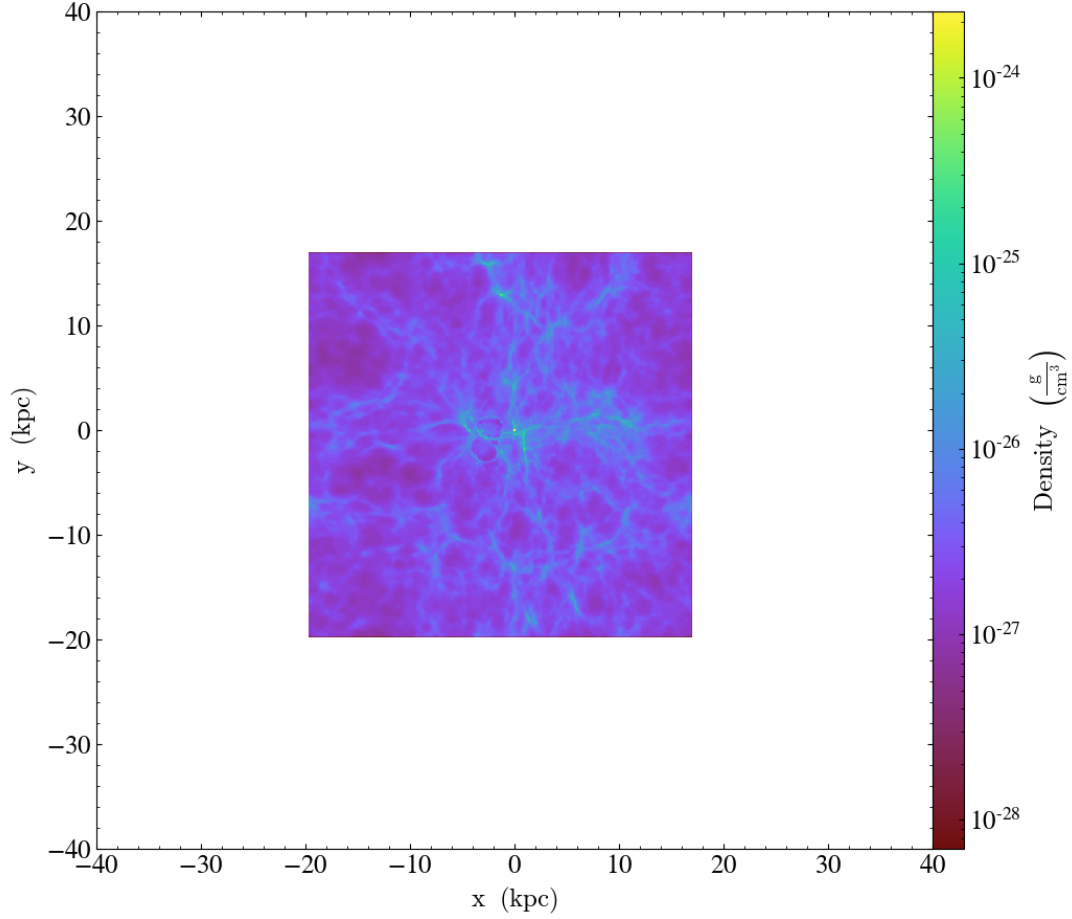


Figure 1: Actual slice of cluster within 20 kpc with density vs distance (kpc)

## 4.2 Multiple slices and radial profiles using python's 'glob'

### *Slices*

Going further, datasets span many directories of information. It is therefore useful to execute iterations that perform slices for multiple directories. This can be done using python's 'glob' as shown.

```
import os
import yt
import glob
import numpy as np
```

```
'''
```

Glob Slice.. This function accesses the wanted directories located in `pisn_solo`, combines them using `glob`, filtering only the directories beginning with `DD0`, returns as a list then sorts the list alphabetically and numerically using `sort`. The function then loops over the list (stored as 'globbed'), and uses `os.path.basename` to replace each element with its base name (last item on its

working directory). For these base names, another for loop is used to load the data set for the appropriate directory and perform the slice using `yt.SlicePlot`. The for loop iterates over an array stored as increasing integers with a png extension and saves each slice for each of the 81 directories located in the `pisn_solo` folder.

```
'''
```

```
def globSlice():
    dat = '/disk12/brs/pop2-prime/firstpop2_L2-Seed3-large/pisn_solo/'
    globbed = glob.glob('/disk12/brs/pop2-prime/firstpop2_L2-Seed3-large/pisn_solo/DD0*')
    globbed.sort()
    for x in globbed:
        y = os.path.basename(x) #strips directories to base name
    for i in y:
        ds = yt.load(os.path.join(dat, "i", "i")) #i is the base name
        plt = yt.SlicePlot(ds, "z", ("gas", "density"), center=("max", "density"), width=(
        plot_directory = '/home/rcanevy/plots/slices' #where to save the file
        name_list = np.arange(1, 81) #list to hold the names of png files, 81 directories
        new_names = tuple(f"{y}.png" for y in name_list) #adds .png extension
    for z in new_names:
        plt.save(os.path.join(plot_directory, z)) #for loop iterates over the list of names

globSlice()
```

Here, the function accesses the wanted directories, combines them into a list using `glob`, filtering only the directories beginning with `DD0`, returns as a list, sorts the list alphabetically and numerically using `sort`. The function loops over the list (stored as `'globbed'`), and uses `os.path.basename` to replace each element with its base name (last item on its working directory). For these base names, another for loop is used to load the data set for the appropriate directory and perform the slice using `yt.SlicePlot`. The third for loop iterates over an array stored as increasing integers with a png extension and saves each slice for each of the 81 directories located in the *pisn\_solo* folder.

The issue here is a 'box' of information is not specific enough as it covers too much area in the one space, instead a 'sphere' of information inside the box can bring into focus points of interest.

In order to do this, `yt` has an in-built key word 'sphere' that can be used, e.g. `mysphere = ds.sphere("c", (100.0, "kpc"))` will create a sphere within 'ds' (the previously defined dataset) located at the centre of the box ("c") at 100 kpc.

### *Radial Profiles*

The same can be done for radial profiles as shown. Utilising glob to collect multiple radial profile plots. Essentially the same as the slice method, but instead 'plt' is assigned to perform profile plots for the average density vs radius.

```
import os
import yt
import glob
import numpy as np
```

```
'''
```

```
Glob Profile plot.. This function accesses the wanted directories located in pism_solo, com
using glob, filtering only the
directories beginning with DD0, returns as a list then sorts the list alphabetically and
numerically using sort. The function then loops over the list (stored as 'globbed'), and
uses os.path.basename to replace each element with its base name (last item on its
working directory). For these base names, another for loop is used to
load the data set for the appropriate directory define a sphere which designates the optim
of interest, loop then performs the radial plot using the in-built yt.ProfilePlot. The thin
for loop iterates over an array stored as increasing integers with a png extension and
saves each profile for each of the 81 directories located in the pism_solo folder, using os
as the path for each png file to be saved in.
'''
```

```
def globProfile():
    dat = '/disk12/brs/pop2-prime/firstpop2-L2-Seed3-large/pism_solo/'
    globbed = glob.glob('/disk12/brs/pop2-prime/firstpop2-L2-Seed3-large/pism_solo/DD0*')
    globbed.sort()
    for x in globbed:
        y = os.path.basename(x) #strips directories to base name
    for i in y:
        ds = yt.load(os.path.join(dat, "i", "i")) #i is the base name
        my_sphere = ds.sphere("c", (100.0, "kpc"))
        plt = yt.ProfilePlot(my_sphere, ("index", "radius"), ("gas", "density"), weight_fie
        # Change the units of the radius into kpc (and not the default in cgs)
        plt.set_unit(("index", "radius"), "kpc")
        plot_directory = '/home/rcanevy/plots/slices' #where to save the file
        name_list = np.arange(1, 81) #list to hold the names of png files, 81 directories l
        new_names = tuple(f"{y}.png" for y in name_list) #adds .png extension
    for z in new_names:
        plt.save(os.path.join(plot_directory, z)) #for loop iterates over the list of names

globProfile()
```

## 5 Ytree

The simulations are modelled using 'ytree', an extension of yt which is used for analyzing merger tree data. Ytree utilizes a function that loads the merger tree data and returns the data as a numpy array that represents the halo. Each halo assigned as an object contains information about its ancestry or descending halos allowing further analysis of the tree one said halo belongs to. Data fields (position, velocity and mass) can be queried for any halo, tree or progenitor line (most massive ancestors). Ytree makes use of the Unyt package assigning field data as subclass objects supported by symbolic units. The ytree package has been used for semi-analytic galaxy formation models following halo trajectories in zoom-in simulations and for studying simulated galaxy properties [20].

### 5.1 Analysis Pipeline

The AnalysisPipeline is the design of the analysis, it is used to process a tree or node within a single function call.

```
import os
import yt
import ytree
yt.enable_parallelism()
import numpy as np

from ytree.analysis import AnalysisPipeline
from yt.extensions.sam_mods.misc import *
from yt.extensions.sam_mods.profiles import my_profile
from yt.extensions.sam_mods.plots import *
from yt.extensions.sam_mods.tree_analysis_operations import yt_dataset, node_profile, garb
from yt.extensions.sam_mods import add_p2p_fields
from yt.extensions.sam_mods.tree_analysis_operations import node_sphere
from yt.extensions.sam_mods import add_p2p_fields
from unyt import unyt_quantity, unyt_array
from unyt import G, Msun, kb, mh, pc

#Optimal bin density for a smooth profile
BIN_DENSITY = 20
#location for profiles to be saved in
OUTDIR = "/home/rcanevy/plots/slices/pipelines/test1"

def sphere_radial_profiles(node, fields, weight_field=None, outdir="."):
    #conditions that ignore an error if the specified field is called as a tuple or not
    if weight_field is None:
        weight_name = "None"
    else:
        if not (isinstance(weight_field, tuple) and len(weight_field) == 2):
            raise ValueError("weight_field must be a tuple of length 2.")
        weight_name = weight_field[1]
    #An f string to correctly name the files (DD00**) with their specified field
    fn = os.path.join(outdir, f"{str(node.ds)}_profile_weight_field_{weight_name}.h5")
    if os.path.exists(fn):
        return
    #attaching a sphere to the node object
```

```

data_source = node.sphere
#perform the profile plot accessing the data source with radius as the x axis in units
#with weight_field set to ignore cell mass and accumulation set to False to avoid an a
weight_field=weight_field , accumulation=False , bin_density=BIN_DE
#save the profile under filename
profile.save_as_dataset(filename=fn)

'''
Contains all profiles to be run
'''
def mass_weighted_profiles(node, outdir="."):

    fields_weighted = [('gas', 'density'),
                       ('gas', 'dark-matter-density'),
                       ('gas', 'matter-density'),
                       ('gas', 'metallicity3'),
                       ('gas', 'H2_p0-fraction'),
                       ('gas', 'temperature'),
                       ('gas', 'pressure'),
                       ('gas', 'entropy'),
                       ('gas', 'sound-speed'),
                       ('gas', 'accretion-rate'),
                       ('gas', 'accretion-rate-z'),
                       ('gas', 'sound-speed'),
                       ('gas', 'vortical-time'),
                       ('gas', 'cooling-time'),
                       ('gas', 'dynamical-time'),
                       ('gas', 'velocity-magnitude'),
                       ('gas', 'total-dynamical-time')]

    fields_raw = [('gas', 'metal3-mass'),
                  ('gas', 'cell-mass'),
                  ('gas', 'matter-mass'),
                  ('gas', 'dark-matter-mass')]

    '''Two lines that call the previous functions fields_weighted lines, setting the weight
    with cell-mass sending the profile to the outdir path specified above. Second line inst
    (the above 2x4 array)
    without a weighted field (no cell mass) and again sending this via outdir (the path to l
    sphere_radial_profiles(node, fields_weighted, weight_field="gas", "cell-mass"), outdir
    sphere_radial_profiles(node, fields_raw, weight_field=None, outdir=outdir)

if __name__ == "__main__":

    # output_dir = "/disk12/brs/pop2-prime/firstpop2-L2-Seed3-large/cc-512-collapse-solar-du
    # sim_path = "/disk12/brs/pop2-prime/firstpop2-L2-Seed3-large/cc-512-collapse-solar-dust
    # data_dir = "/disk12/brs/pop2-prime/firstpop2-L2-Seed3-large/cc-512-collapse-solar-dust
    # tree_path = "/disk12/brs/pop2-prime/firstpop2-L2-Seed3-large/cc-512-collapse-solar-dust

    output_dir = "/disk12/brs/pop2-prime/firstpop2-L2-Seed3-large/pisn-solo/minihalo-analy
    sim_path = "/disk12/brs/pop2-prime/firstpop2-L2-Seed3-large/pisn-solo/simulation.h5"

```

```

data_dir = "/disk12/brs/pop2-prime/firstpop2_L2-Seed3-large/pisn-solo"
#path to file containing dark matter tree information
tree_path = "/disk12/brs/pop2-prime/firstpop2_L2-Seed3-large/pisn-solo/merger-trees/ta

es = yt.load(sim_path)
#load tree file
a = ytree.load(tree_path)
#Conditional to add a vector field as position
if "icom_gas2_position_x" in a.field_list:
    a.add_vector_field("icom_gas2_position")
#define variable ap as the pipeline object
ap = AnalysisPipeline()
#use keyword add_operation to; add the dataset, the p2p fields, the node_sphere (centre
#mass-weighted profiles added and sent to the correct path
ap.add_operation(yt_dataset, data_dir, add_fields=True) #uses the time of a halo within
#ap.add_operation(add_p2p_fields)
#ap.add_operation(node_sphere, center_field="icom_gas2_position")
ap.add_operation(return_sphere)
ap.add_operation(align_sphere)
ap.add_operation(mass_weighted_profiles, outdir=OUTDIR)

ap.add_operation(delattrs, ["sphere", "ds"], always_do=True) #deletes any attributes no
ap.add_operation(garbage_collect, 60, always_do=True) #deletes any attributes no longer

tree = a[0]
for node in ytree.parallel_tree_nodes(tree, group="prog"):
    ap.process_target(node)

```

### *Pipeline Description*

The pipeline designed for this report was a collection of 17 different spherical radial profiles, all with gas. The code begins with a function that bypasses whether a field is specified within a tuple, names the file using an f string, attaches a sphere to the chosen node, performs the profile with the radius as the x axis, assigns the weight field to ignore cell mass, assigns the accumulation to False to bypass an accumulative graph and saving the plot.

Stored in 'fields weighted', the 13 weighted fields included density, dark matter density component, density of matter, metallicity, H2 fraction, temperature, pressure, entropy, sound speed, accretion rate, z axis accretion rate, sound speed again, vortical time (as per the formula), cooling time, dynamical time (also known as the free fall time), magnitude of velocity and the total dynamical time for the halo.

The non-weighted fields labelled 'raw' with gas were metal mass, cell mass, matter mass and dark matter mass for the halo.

The final section beginning with a conditional statement, defines the path to where the data for the tree is saved. The tree is loaded, the analysis pipeline is defined and multiple functions are added to the pipeline; the dataset, mass weighted profiles, delattr and garbage collect. The section concludes with a filter, *selection*, assigned to the in-built function *get\_yt\_selection*, an enhanced functionality returning a data container that is queried for the value of the field, it can then be used to generate the tree nodes. The filter for this pipeline returns redshifts near 18.22 with uncertainty 0.2, with  $M > 1e^5 M_\odot$  mass above 1e5 solar masses

The pipeline will return a set of 100 or so files ending in .h5 to the specified out directory. An appropriate python script can then be executed for one or multiple (glob) files to plot the weighted or non weighted fields as listed in the mass weighted profiles function.



```

import matplotlib.pyplot as plt
import yt
import os

plot_directory = '/home/rcanev/plots/slices/pipelines/test1'
sample_plot = 'pre.png'
path = os.path.join(plot_directory, "000265_profile_weight_field_cell_mass.h5")
ds = yt.load(path)
plt.plot(ds.data[('data', 'radius')], ds.data[('data', 'metallicity')])
plt.xlabel('Radius (kpc)')
plt.xlim(0, 400)
plt.ylabel('Metallicity (solar Z)')
plt.savefig(os.path.join(plot_directory, sample_plot))

```

(a) Single Metallicity Profile

```

import matplotlib.pyplot as plt
import yt
import os

plot_directory = '/home/rcanev/plots/slices/pipelines/test1'
sample_plot = 'vortical.png'
path = os.path.join(plot_directory, "000265_profile_weight_field_cell_mass.h5")
ds = yt.load(path)
plt.loglog(ds.data[('data', 'radius')], ds.data[('data', 'vortical_time')], label = 'log Vortical Time')
plt.loglog(ds.data[('data', 'radius')], ds.data[('data', 'cooling_time')], label = 'log Cooling Time')
plt.loglog(ds.data[('data', 'radius')], ds.data[('data', 'dynamical_time')], label = 'log Dynamical Time')
plt.xlim(10**0, 340)
plt.xlabel('log radius (kpc)')
plt.ylabel('Time (yr)')
plt.savefig(os.path.join(plot_directory, sample_plot))

```

(b) Single Vortical, Cooling Dynamical Time

Figure 2: Script for creating a single plot for a metallicity profile a) and vortical, cooling, dynamical time profiles b)

```

import os
import yt
import glob
import numpy as np
import matplotlib.pyplot as plt

...
This function processes the sorted directories located in dat, combines them into a list using glob, filtering only the
directories beginning with 000, returns as a list then sorts the list alphabetically and
numerically using sort.
The function then loops over the list (stores as 'globbed'), and
uses os.path.basename to replace each element with its base name (last item on its working directory).
For each base name, for loop1 used to load the data set for that file.
The second for loop iterates over an array stored as increasing integers with a
log extension and saves each plot for each of the ".h5" files located in the 'dat' folder.

def globnet():
    dat = '/home/rcanev/plots/slices/pipelines/test1'
    fold = '/home/rcanev/plots/slices/pipelines/test1/globnet/'
    globbed = glob.glob('%s/%s' % (dat, '*000*'))
    globbed.sort()
    print(globbed)
    for x in globbed:
        y = os.path.basename(x) #strip directories to base name
        print(y)
        ds = yt.load(os.path.join(dat, y))
        plt.figure()
        plt.plot(ds.data[('data', 'radius')], ds.data[('data', 'metallicity')])
        plt.xlabel('Radius (kpc)')
        plt.ylabel('Metallicity (Z_sun)')
        name_list = np.arange(1, 50) #list to hold the names of figs
        new_names = [] #list to hold the new names of figs
        for i in range(1, 50):
            for i in name_list:
                new_names.append('%s_%s' % (y, i))
        for i in new_names:
            plt.savefig(os.path.join(fold, i)) #for loop iterates over the list of names, and saves the slices
            plt.close()
    globnet()

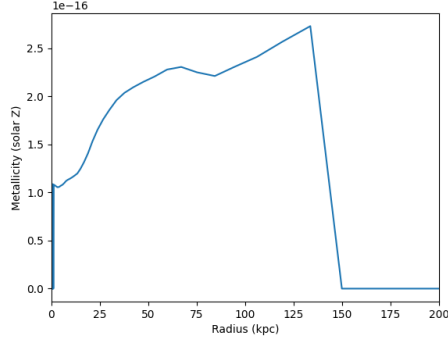
```

(a) Multi-Metallicity Profiles

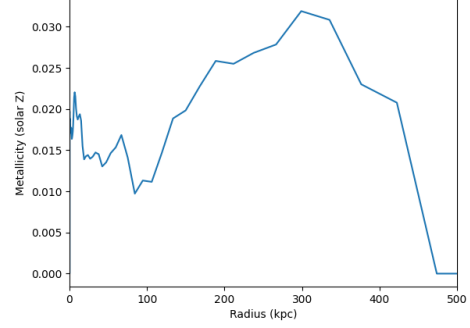
Figure 3: Script for performing multiple metallicity profiles on a specified directory

## 6 Analysis Pipeline Results

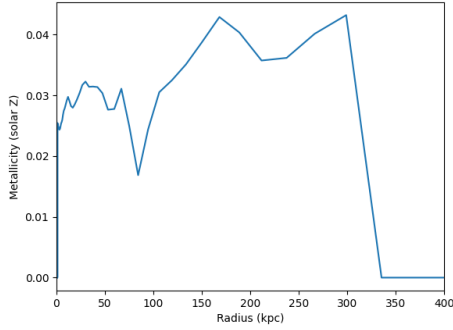
### 6.1 Metallicity Profiles



(a) Internally Enriched



(b) Externally Enriched



(c) Pre-Enriched

Figure 4: Metallicity profiles for the halo at a) Internally Enriched, b) Externally Enriched and c) Pre-Enriched. Binning adjusted with distance from centre, each bin contains a mass weighted average for the metallicity [1]

## 6.2 Vortical Time

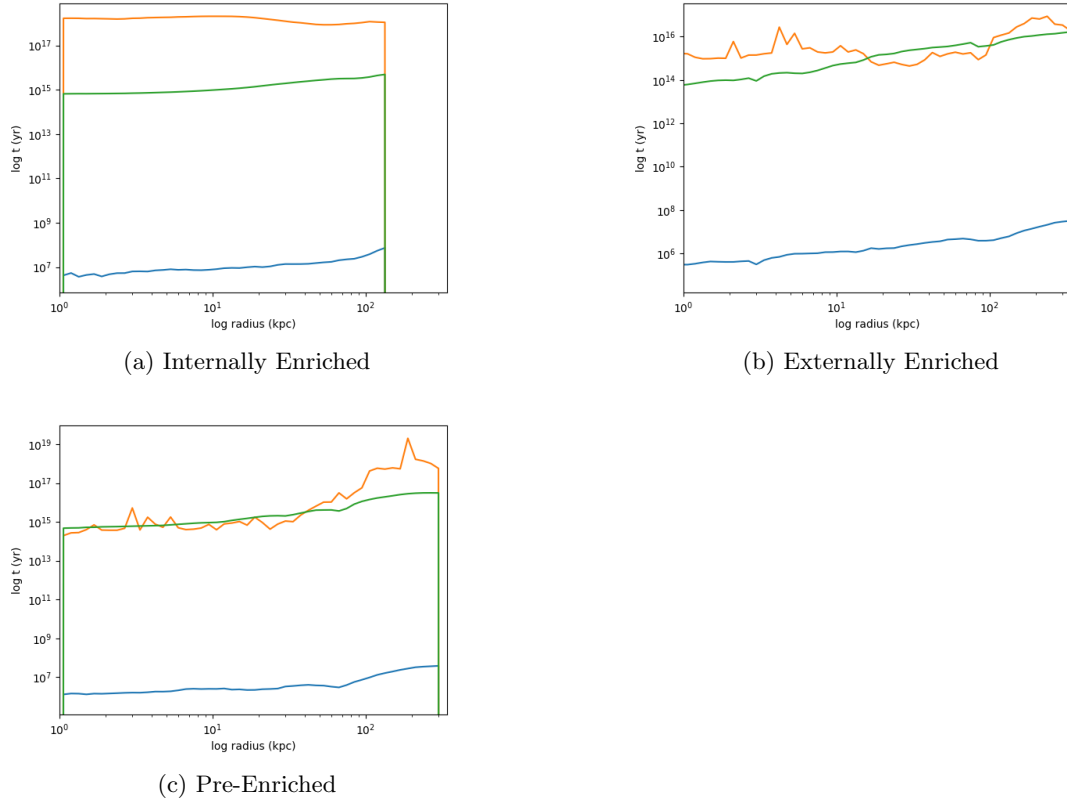


Figure 5: Vortical (Blue), Cooling (Orange) and Dynamical time (Green) plots for the halo during a) Internally Enriched, b) Externally Enriched and c) Pre-Enriched phases [1]

## 7 Discussion

From [1] *Hicks et al* fragmentation, internal enrichment occurs within the centre of the halo. From Figure 4 a), the metallicity profile shows an increase in  $Z_{\odot}$  towards the centre, followed by a sharp decrease approaching the virial radius. Figure 4 b) depicts a climb demonstrating EE where a hypernova event outside the virial radius occurs. Due to turbulent mixing the highest values are located at the edge of the halo and lower values towards the centre. Figure 4 c) shows Pre-Enrichment for a halo forming in a region already enriched via PISNe, where the metal over a period of time has already mixed with the surroundings indicating a flat metallicity profile is to be expected [1].

From Figure 5, the efficiency of how well mixing that arises from turbulence occurs can be seen from the off-set of the vortical time line and the dynamical or cooling time lines.

Turbulence results in the efficient mixing of metals over the length scales of the turbulent cascade which are comparable to the local dynamical time in supersonic turbulence [3].

## 8 Conclusion

An analysis pipeline was constructed to provide 50 or so different datasets each containing mass weighted fields and non weighted fields. Focusing on the mass weighted fields; metallicity, vortical time, cooling time and dynamical time - profiles were constructed to investigate the enrichment mechanism and mixing efficiency respectively. This material emphasises information from Hicks et al [1] where the number of both internally and externally enriched halos increases over time - as redshift decreases, external enrichment becomes the most common enrichment vector. [1]. The efficiency of the mixing induced by turbulence was also confirmed in the EE mechanism.

Over the previous decade, mixing brought on by turbulence from the SNe is a relatively recent confirmation, the importance of how efficient it occurs within given mechanisms of enrichment has been a very significant factor in the given field. With the aid of magnetohydrodynamical formulae solved by Enzo and recent developments, our knowledge of this mixing has the potential to grow even further in upcoming analysis of the primordial Universe.

## References

- [1] W. M. Hicks et al., “External enrichment of mini halos by the first supernovae”, *The Astrophysical Journal* **909**, 70 (2021).
- [2] M. L. Norman et al., “Simulating the cosmic dawn with enzo”, *Frontiers in Astronomy and Space Sciences* **5**, 34 (2018).
- [3] B. D. Smith et al., “The first population ii stars formed in externally enriched mini-haloes”, *Monthly Notices of the Royal Astronomical Society* **452**, 2822–2836 (2015).
- [4] G. Chiaki et al., “Metal-poor star formation triggered by the feedback effects from pop iii stars”, *Monthly Notices of the Royal Astronomical Society* **475**, 4378–4395 (2018).
- [5] G. Chiaki et al., “Seeding the second star: enrichment from population iii, dust evolution, and cloud collapse”, *Monthly Notices of the Royal Astronomical Society* **482**, 3933–3949 (2019).
- [6] V. Bromm et al., “The first stars”, *Annu. Rev. Astron. Astrophys.* **42**, 79–118 (2004).
- [7] J. H. Wise et al., “The birth of a galaxy: primordial metal enrichment and stellar populations”, *The Astrophysical Journal* **745**, 50 (2011).
- [8] J. Tumlinson, “Near-field cosmology and the first stars: insights from chemical evolution”, *New Astronomy Reviews* **50**, 101–107 (2006).
- [9] C. Bertulani et al., “Frontiers in nuclear astrophysics”, *Progress in Particle and Nuclear Physics* **89**, 56–100 (2016).
- [10] S. Planelles et al., “Cosmological shock waves: clues to the formation history of haloes”, *Monthly Notices of the Royal Astronomical Society* **428**, 1643–1655 (2013).
- [11] G Rakavy et al., “Instabilities in highly evolved stellar models”, *The Astrophysical Journal* **148**, 803 (1967).
- [12] J. A. Regan et al., “Pathways to massive black holes and compact star clusters in pre-galactic dark matter haloes with virial temperatures 10 000 k”, *Monthly Notices of the Royal Astronomical Society* **396**, 343–353 (2009).
- [13] U. Maio et al., “The interplay between chemical and mechanical feedback from the first generation of stars”, *Monthly Notices of the Royal Astronomical Society* **414**, 1145–1157 (2011).
- [14] T. H. Greif et al., “The first galaxies: chemical enrichment, mixing, and star formation”, *The Astrophysical Journal* **716**, 510 (2010).
- [15] O. Ibe, *Markov processes for stochastic modeling* (Newnes, 2013).
- [16] I. T. Iliev et al., “Cosmological radiative transfer comparison project–ii. the radiation-hydrodynamic tests”, *Monthly Notices of the Royal Astronomical Society* **400**, 1283–1316 (2009).

- [17] S. Shen et al., “The enrichment of the intergalactic medium with adiabatic feedback–i. metal cooling and metal diffusion”, *Monthly Notices of the Royal Astronomical Society* **407**, 1581–1596 (2010).
- [18] V. Bromm et al., “Formation of the first supermassive black holes”, *The Astrophysical Journal* **596**, 34 (2003).
- [19] G. L. Bryan et al., “Enzo: an adaptive mesh refinement code for astrophysics”, *The Astrophysical Journal Supplement Series* **211**, 19 (2014).
- [20] B. D. Smith et al., “Ytree: a python package for analyzing merger trees”, *Journal of Open Source Software* **4**, 1881 (2019).